АТОМНА ЕНЕРГЕТИКА
ATOMIC ENERGY

УДК 621.039 https://doi.org/10.15407/jnpae2026.01.026

V. A. Babenko[1,2,*], V. M. Pavlovych[1], I. A. Khomych[1], V. I. Slisenko[1], V. V. Tryshyn[1], O. P. Volokh[1]

[1] *Institute for Nuclear Research, National Academy of Sciences of Ukraine, Kyiv, Ukraine*
[2] *Bogolyubov Institute for Theoretical Physics, National Academy of Sciences of Ukraine, Kyiv, Ukraine*

*Corresponding author: pet2@ukr.net

SAMPLE IRRADIATION MODELING AND NUCLEAR SAFETY JUSTIFICATION AT THE WWR-M RESEARCH REACTOR

We have analyzed the activities conducted at the WWR-M nuclear research reactor of the Institute for Nuclear Research, NAS of Ukraine, over the past five years, with a focus on nuclear safety and ongoing research efforts. In 2019–2022, preparatory work was carried out for the irradiation of surveillance specimens of nuclear power reactor vessel metals in the vertical channels of the WWR-M reactor, commissioned by the National Nuclear Energy Generating Company (NNEC) "Energoatom". To support this effort, vertical channels for sample irradiation were designed and manufactured, and computational analyses were performed to determine the optimal core configuration, the optimal placement of channels within the core, neutron flux distributions, and the required irradiation time. The research presented here is based on computational modeling using the MCNP-4C code, with calculations performed to evaluate neutron fluxes, reactivity parameters, and nuclear safety margins. For each configuration, critical nuclear safety parameters were determined, including the reactivity margin, the control rod worth, the reactivity of the irradiated channels, and that of each fuel assembly. The analysis confirmed the feasibility of the proposed configuration and provided essential insights into optimizing neutron flux distributions and reactivity control. In early 2022, all reactor operations were halted, and the fuel was removed from the core and transferred to storage facilities. As a result, the need arose to improve the nuclear safety justification for the spent nuclear fuel storage facility, taking into account the actual arrangement of fuel assemblies. The present work examines reactor safety considerations and explores approaches to improving the justification of spent fuel storage. It also presents the results of a series of such calculations that were initiated and remain ongoing. Overall, our research contributes to current efforts in nuclear safety assessment and provides a foundation for future investigations in this field.

Keywords: WWR-M research reactor, fuel assembly, nuclear fuel, storage facility.

1. Introduction

The WWR-M research nuclear reactor, a water-moderated water-cooled modernized research reactor at the Institute for Nuclear Research of the National Academy of Sciences of Ukraine (Kyiv) (INR of NASU), was put into operation in 1960. It is a pool-type reactor where water serves as a neutron moderator and coolant, also forming the primary component of the biological shielding (Fig. 1).

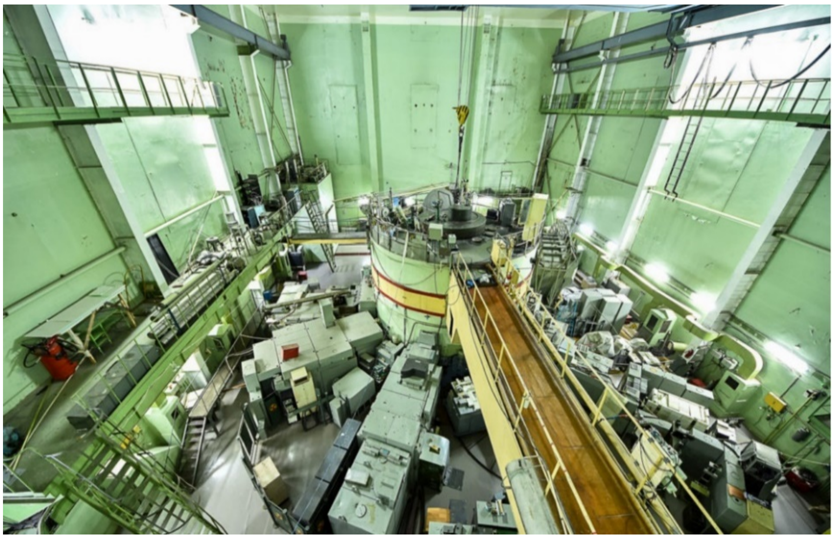

Fig. 1. General view of the WWR-M research nuclear reactor.
(See color Figure on the journal website.)

© The Author(s), 2026
Published by INR of NAS of Ukraine as an open access article under the CC BY-NC 4.0 license

Its main technical characteristics are as follows [1]: the reactor has a power of 10 MW; the maximum thermal neutron flux reaches $1.2 \cdot 10^{14}$ n/cm²·s; the maximum fast neutron flux reaches $0.7 \cdot 10^{14}$ n/cm²·s; the nuclear fuel used is uranium dioxide UO_2 in an aluminum matrix; after 2011, the enrichment level was 19.7 % (before 2011, it was primarily 36 %); the number of fuel assemblies per unit ranges from 156 to 252; the control and protection system includes 3 emergency protection rods, 5 compensating rods, and one automatic regulation rod; the neutron absorber in the rods is B_4C, while the fine regulation rod uses stainless steel; the neutron reflector material is beryllium. The reactor core configuration includes fuel assemblies as well as beryllium and aluminum displacers.

The reactor cooling system operates as a two-loop system, where the primary loop utilizes distilled water; the maximum water level in the reactor tank reaches 5100 mm; the water flow rate in the primary loop is at least 1250 m^3/h; the water pressure after the primary loop pumps is no less than 0.15 MPa; the water temperature at the reactor core outlet does not exceed 55 °C; the temperature difference across the reactor core is up to 6.9 °C; the water flow rate in the secondary loop is at least 900 m^3/h; the water pressure in the secondary loop ranges between 0.2 and 0.4 MPa; the water temperature in the secondary loop before the heat exchangers is no more than 35 °C [1].

The WWR-M research reactor is equipped with various devices for irradiating samples and targets with neutrons and gamma quanta of different energies. In particular, it features 9 horizontal experimental channels and a graphite thermal column; 13 vertical channels embedded in the beryllium reflector; 4 vertical channels located in the thermal column; and 3 vertical channels positioned within the biological shielding. Irradiation can also be conducted directly in the reactor core by replacing fuel assemblies with vertical channels or special irradiation devices.

To study irradiated samples and manipulate irradiated materials, the reactor is equipped with four "hot" cells, one of which provides direct access to the reactor interior. Later, an additional eight "hot" cells were put into operation, primarily intended for materials research. They are connected to the standard cells through a remote transport system.

Over the past 60-plus years, a vast number of fundamental and applied studies have been conducted at the WWR-M reactor in the fields of nuclear, neutron, and radiation physics, as well as reactor physics and engineering, radiation materials science, solid-state and liquid physics, radiation biology, medicine, and ecology [2–4]. These studies have been published in both national and international scientific journals. Among the applied studies, notable research includes work on neutron doping of silicon [5]; testing of in-reactor monitoring sensors, particularly direct charge detectors and calorimeters [6]; investigations on radiation resistance and high-temperature embrittlement of structural materials for nuclear reactors [7]; development of technologies for producing radioactive isotopes for medical and industrial applications [8]; and neutron activation analysis of various geological and environmental samples. Preventive maintenance, repair work, and modernization of various reactor complex systems were also performed.

Particular attention should be given to research focused on providing scientific support for all studies related to the irradiation of various materials and samples with neutrons and reactor gamma rays, both inside the reactor core and in external channels. These activities are carried out on an ongoing basis throughout the reactor's operational lifetime and involve determining the optimal fuel reloading design for specific tasks; calculating neutron flux density in each fuel assembly and, preferably, in each irradiated sample; evaluating reactivity margin for each reloading cycle; estimating the control rod worth; burnup estimates for each assembly; and ensuring the nuclear safety of all possible core configurations.

In this paper, we briefly outline the results of studies conducted at the Kyiv WWR-M research reactor over the past five years. Specifically, between 2020 and 2022, the authors were involved in the preparation of surveillance specimens (commonly referred to as witness samples in local practice) for irradiation in the vertical channels of the WWR-M reactor, as part of a project commissioned by the State Enterprise "National Nuclear Energy Generating Company (NNEC) "Energoatom". Additionally, work was carried out to ensure the nuclear safety of the spent nuclear fuel storage facility, where fuel from the reactor core was relocated in the spring of 2022. Thus, the present manuscript reports two closely related parts of research conducted at the WWR-M reactor over the past five years: (i) computational support of surveillance-specimen irradiation in vertical channels, and (ii) follow-up nuclear safety justification calculations for spent fuel storage performed after the 2022 shutdown. Both parts rely on the same MCNP-4C modeling framework.

2. Irradiation of surveillance specimens of structural materials for nuclear power reactors

Currently, the projected operational lifetime of the metal pressure vessels of WWER-type nuclear reactors is determined based on the evaluation of T_c, the critical brittle fracture temperature of the reactor vessel metal under irradiation by fast neutrons ($E > 0.5$ MeV) at a fluence corresponding to the specified operational period of the reactor at nominal power. This evaluation, in turn, is derived from the findings of experimental and computational research using surveillance specimens, which consist of steel specimens taken from the reactor vessel during its fabrication, as well as from the welds connecting its sections. These specimens are placed in a specialized container that also accommodates neutron activation detectors for neutron fluence, with the container located inside the reactor vessel, usually above the core. Following each reactor fuel cycle, a portion of the surveillance specimens is extracted from the reactor, and specialized mechanical testing is conducted to evaluate the variation in brittle fracture temperature as fluence increases [9–14].

The above approach has certain limitations, with the primary issue being that the neutron fluence on the surveillance specimens is significantly lower than that on the reactor vessel, particularly in areas where the neutron flux reaches its maximum, namely, the regions directly opposite to the core center. Providing a comprehensive review of the limitations of the T_c evaluation method is beyond the scope of this paper. We only note in this context that irradiating (or re-irradiating) the surveillance specimens to a fluence level corresponding to the maximum actual fluence on the reactor vessel is a highly desirable addition to the standard surveillance specimen methodology for reliably assessing the feasibility of extending the operational lifetime of nuclear power reactor vessels.

As part of this initiative, the INR of NASU launched preparations in 2020 for the irradiation of surveillance specimens at the WWR-M reactor under a project commissioned by NNEC "Energoatom". The preparation process included the following phases. (1) The development and manufacturing of a vertical channel and a set of irradiation containers for surveillance specimens within the WWR-M reactor core, located at one of the fuel assembly positions. As part of this effort, it was decided to manufacture an additional irradiation channel for surveillance specimens and to conduct irradiation simultaneously in both channels. (2) Calculation of neutron fluxes and the optimal reactor core configuration, considering the fuel assembly burnup status at the time of calculation. (3) Nuclear safety studies of the selected configuration, specifically the calculation of the reactivity margin and the worth of emergency and control rods, as well as the experimental determination of these parameters directly in the reactor.

Fig. 2. Photographs of the material science vertical irradiation channels for irradiating surveillance specimens in the WWR-M reactor core: *a* - the smaller-diameter channel designed for a single fuel assembly; *b* - the larger-diameter channel designed for a triple fuel assembly.

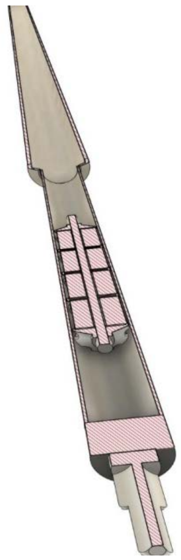

Fig. 3. Schematic diagram of the surveillance specimen container inside the first vertical irradiation channel (single fuel assembly position). (See color Figure on the journal website.)

The dry vertical irradiation channel for surveillance specimens is a hermetically sealed stainless-steel unit, connected at the top to a gas compression station for the flow of cooling helium (Fig. 2). It was designed and manufactured by order of NNEC "Energoatom". This channel is installed within the reactor core at the location of one of the fuel assemblies, with its placement determined based on neutron flux calculations for various core configuration options. The second vertical channel, which has a slightly different design, is placed in the position of a triple assembly (see Fig. 2). The surveillance specimen container is positioned inside the channel at the reactor core midplane (Fig. 3). In what follows, we consider the first vertical channel (single fuel assembly position), into which the container with surveillance specimens is inserted. The temperature of the surveillance specimens is monitored by thermocouples, while the containers holding the specimens are cooled using helium.

Let us now consider various neutron flux calculations. In recent years, the well-known MCNP-4C transport code has been used for all calculations of reactor characteristics [15]. A detailed computational model of the reactor was developed for these calculations [16–18], enabling criticality evaluation and neutron flux calculations in all reactor channels (horizontal and vertical), as well as within the reactor core. This model can be visualized using the MCNP-VISED code. An example of such visualization is presented in Fig. 4, illustrating the preliminary calculation model for the irradiation channel installation at the location of one of the fuel assemblies.

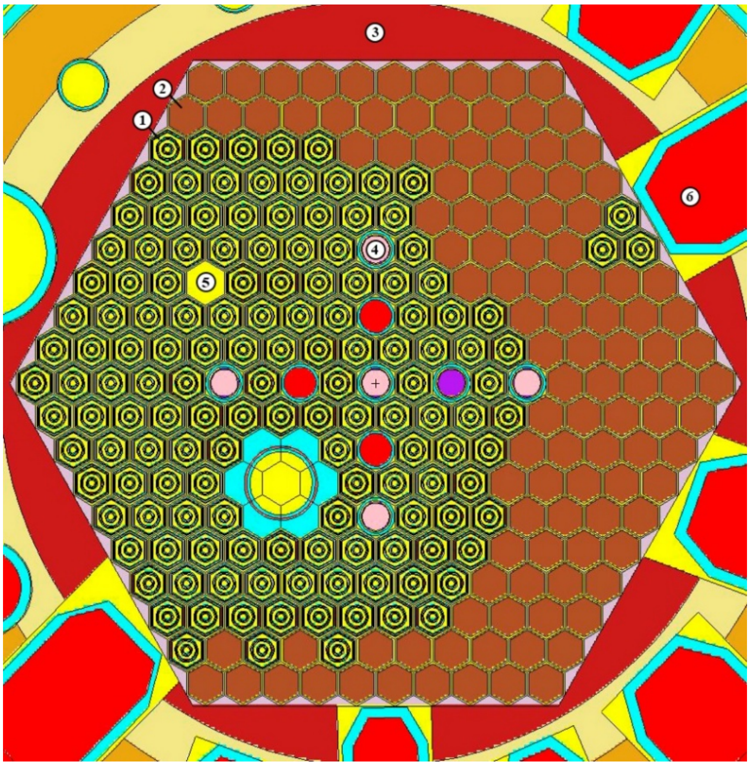

Fig. 4. Example of the visualization of the computational model of the WWR-M reactor core used in this study. The view shows the reactor core layout, with labeled elements including fuel assemblies (*1*), beryllium displacers (*2*), beryllium reflector (*3*), control and emergency rods (*4*), vertical irradiation channels (*5*), and horizontal experimental channels (*6*). (See color Figure on the journal website.)

Fig. 4 shows a horizontal cross-section of the reactor core at half its height. The hexagonal reactor core is enclosed within the beryllium reflector. The three shades of beryllium indicate different degrees of beryllium contamination by neutron transmutation products. The reflector partially reveals three vertical dry channels (red color – air) and three vertical wet channels (yellow color – water), as well as three horizontal channels leading to the experimental hall, totaling nine channels. There is also a tenth horizontal channel passing through the graphite thermal column. The core contains a hexagonal lattice of fuel assemblies and beryllium displacers, a cross-shaped arrangement of control and emergency protection rods, a dry vertical irradiation channel, and a "chamomile" device for exposing other samples to thermal neutrons.

All calculations of the appropriate core configuration and the selection of the location for the vertical channel used for irradiating surveillance specimens were carried out taking into account the fuel burnup relevant at the time of calculation. This burnup was evaluated using a simplified approach that allows the calculation of the average burnup of a group of fuel assemblies loaded simultaneously into the core and taken into account in the formation of each new configuration. After the transition to low-enriched fuel with 19.7 % enrichment in 2011, a total of seven such loadings were performed. For each reactor core configuration (number), the energy output over the entire operating period of that core is recorded.

Based on the information about the number of assemblies in the core, the energy output of each core configuration, and the known value of the energy released during the fission of a single uranium nucleus by thermal neutrons, the average burnup of a group of assemblies can be calculated.

The results of the calculations of the average fuel burnup

$$B = (m_{burned}/m_0)\cdot 100\ \%,$$

where m_{burned} is the amount of ^{235}U burned in a given assembly, and m_0 is the initial amount of uranium in the assembly ($m_0 = 41.7$ g in each single fresh fuel assembly), are presented in Table 1. Note that the last two rows in Table 1 (m_{burned} and B) are not per-campaign parameters; they characterize the fuel assemblies loaded in the given configuration and are evaluated using cumulative data up to configuration 402. In this case, we also consider that

$$M_{burned} = 1.23\ Q.$$

Table 1. **Average burnup of assembly groups**

Reactor core number	396	397	398	399	400	401	402
N_i – Number of fuel assemblies in the core (converted to single assemblies)	72	85	88	96	101	121	129
Heat generation Q (MW·day)	7.77	97.15	0.48	67.7	4.49	10.57	12.5
M_{burned}, g	9.55	119.49	0.59	83.27	5.52	13.00	15.37
m_{burned}^i, (g) = M_{burned}/N_i	0.13	1.41	0.0067	0.87	0.054	0.11	0.12
$m_{burned} = \Sigma\ m_{burned}^i$	2.707	2.5807	1.1607	1.154	0.284	0.23	0.12
$B = (m_{burned}/m_0)\cdot 100$ %	6.5	6.2	2.8	2.7	0.7	0.6	0.2

Here, M_{burned} denotes the total mass of ^{235}U burned in the core (g), and Q is the total heat generation of the core (MW·day). However, this estimate does not account for several factors. (1) It does not take into account the fission of plutonium, which is produced in the reactor when a ^{238}U nucleus absorbs a neutron. (2) As is known, the reactor neutron spectrum is not purely thermal; it also contains intermediate and fast neutrons, which affect energy release and radiative capture reactions. (3) The presented estimates give only the average burnup for the entire group of assemblies located in the core. The burnup of each fuel assembly is determined by the neutron distribution and depends on its location in the core. Assemblies at the edge of the core undergo lower burnup than those located in the center. Moreover, there is a significant nonuniformity of burnup along the height of the assembly.

The last two rows (m_{burned} and B) characterize the fuel assemblies loaded in the given configuration and represent average per-assembly values derived from the cumulative core heat generation up to configuration 402; they are not per-campaign parameters.

Thus, for the first 72 assemblies that were used in the reactor throughout its entire operation with low-enriched fuel, the burnup reached 6.5 %. At the same time, the first 18 low-enriched fuel assemblies were loaded into the highly enriched core to be exposed to neutrons in order to generate at least a small amount of transuranic elements that emit spontaneous neutrons. Given that such "neutron exposure" caused 7 assemblies to initially have a burnup of 2 %, while 11 assemblies had an initial burnup of 1 %, the core now contains 7 assemblies with a burnup of 8.5 %, 11 assemblies with a burnup of 7.5 %, and 54 assemblies with a burnup of 6.5 %. The next 13 assemblies, which were loaded to form the 397th core configuration, have a burnup of 6.2 %; 3 assemblies (one triple assembly, 398th core configuration) have a burnup of 2.8 %; 8 assemblies (399th core configuration) have a burnup of 2.7 %; 5 assemblies (400th core configuration) have a burnup of 0.7 %; 20 assemblies (401st core configuration) have a burnup of 0.6 %; and 8 assemblies (402nd core configuration) have a burnup of 0.2 %.

Once again, we emphasize that we have calculated the average burnup of the assemblies loaded into the reactor core. The actual burnup of each assembly is determined by the neutron flux density distribution in the reactor core, varies along the assembly height, and depends on its position. The neutron flux density distribution in the horizontal plane will be calculated below for a specific reactor core configuration, while its vertical distribution is known from theoretical considerations and is approximately described by a function $\Phi = \Phi_0 \cos\left(\frac{\pi}{2} z / H\right)$. This formula represents the classical model of neutron flux distribution in the vertical direction in thermal nuclear reactors with a cylindrical core geometry. Given that the mean value of the function cos(x) is 1/2, it follows that the burnup inside each assembly is roughly twice the average.

Fuel burnup is not merely the reduction of ^{235}U content (although the fuel burnup percentage is determined precisely by the decrease in ^{235}U amount), but also involves the accumulation of transuranic elements and fission products, i.e., it represents a change in the isotopic composition of the fuel. The calculation of fuel isotopic composition changes is a separate task that can be solved using ORIGEN or SERPENT codes, or other similar tools. In the present study, to account for fuel burnup in the calculations, we will rely on the results of [18], where the author conducted computations of the isotopic composition of 19.7 % enriched fuel for burnup values of 0, 10, 20, 30, 40, and 50 % in a reactor core exposed to a thermal neutron flux of 10^{14} n/cm^2·s. In the case of intermediate burnup values, the nuclear concentrations of various isotopes can be estimated using linear interpolation of these data, although this method does not provide perfect accuracy. As a result, the calculations use the isotopic composition of burned fuel, which includes 39 stable or long-lived fission product isotopes. Going forward, we intend to refine the data on burnup and the isotopic composition of spent fuel.

The optimization of the placement of the sample irradiation channels in the reactor – specifically, two such channels operating simultaneously – involves three key factors. (1) Selecting locations in the reactor core where the neutron flux is sufficient for long-term irradiation of samples in both channels, while ensuring that neutron flux differences between them remain minimal. (2) Ensuring that the selected locations allow easy access to communication lines and maintenance during irradiation. (3) Guaranteeing the safe operation of the reactor with a sufficient reactivity margin to support prolonged sample irradiation. Before performing the calculations to justify the placement of the sample irradiation channels, it was necessary to develop computational models for both the WWR-M reactor core and the sample irradiation channels themselves. The drawings of the channels, as well as the chemical composition of the materials used for their fabrication, were provided by the customer. The computational model of the irradiation containers (three variants), as well as that of the samples, features a simplified geometry but an accurate chemical composition of the materials and precise vertical placement within the experimental channel.

The locations of the irradiation channels were selected in the upper-left quadrant of the standard core map of the WWR-M reactor. To refine the cell locations of the experimental channels in this quadrant, the neutron flux was calculated for the current reactor core configuration (loading 403). Based on the calculations, two configurations for the placement of the experimental channels were chosen, as shown in Figs. 5 and 6. These figures illustrate the current arrangement of the fuel assemblies, which is not final.

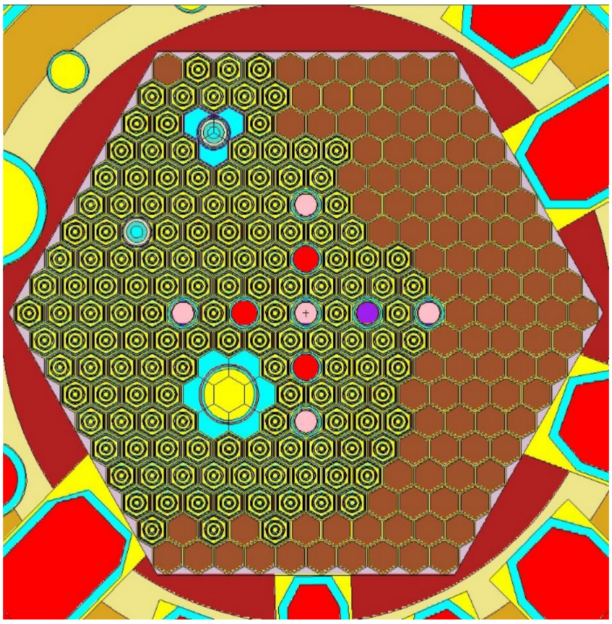

Fig. 5. Variant 1 of channel placement in the reactor core. (See color Figure on the journal website.)

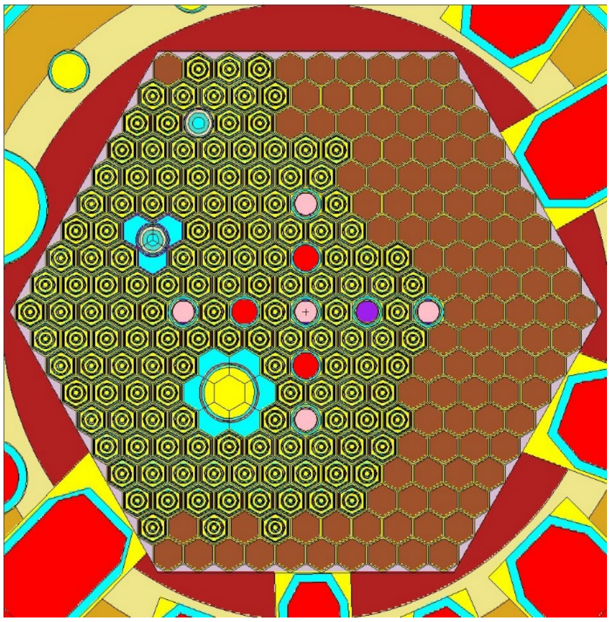

Fig. 6. Variant 2 of channel placement in the reactor core. (See color Figure on the journal website.)

Neutron flux calculations were performed for the selected configurations, with the results presented in Figs. 7 and 8. These figures display the total neutron flux only at the positions of the channels. Overall, the main characteristics influencing nuclear safety were calculated for about 50 different reactor core configurations. These properties include subcriticality, reactivity margin, the control rod worth, the "worth" of experimental channels, and similar parameters. Neutron fluxes were computed for approximately 20 of these configurations. In our estimates of irradiation time and radiation damage, we used the fast neutron flux ($E > 0.5$ MeV) at the sample center; for the considered configurations, its spatial trend is fully consistent with the total-flux trend shown in Figs. 7 and 8. For reference, in variant 2, this fast-neutron flux at the sample positions is $(2.54–2.67)\cdot10^{13}$ n/cm^2·s, i.e., about 30 % of the corresponding total flux.

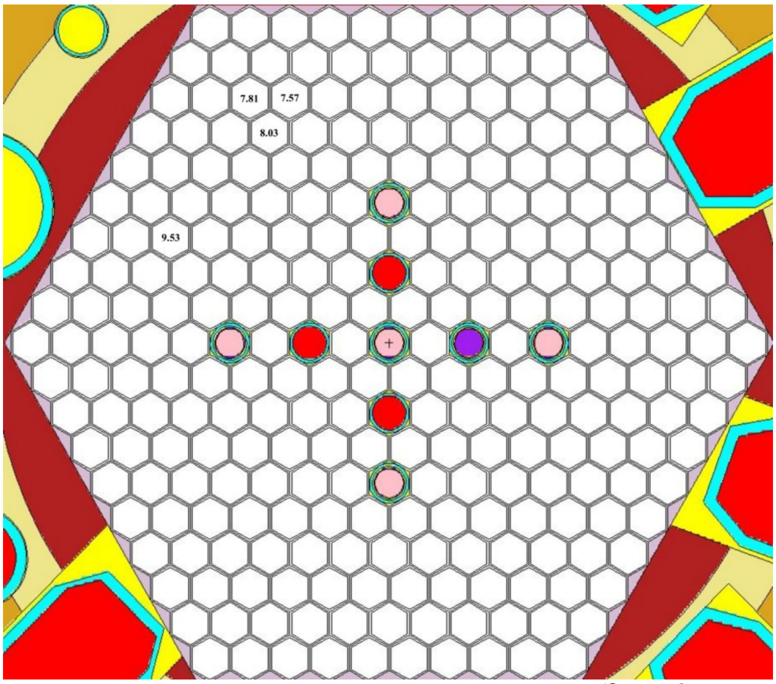

Fig. 7. Total neutron fluxes for variant 1 of channel placement, in units of 10^{13} n/cm^2·s. For irradiation planning, the fast-neutron component (> 0.5 MeV) governing sample damage was used (see the text). (See color Figure on the journal website.)

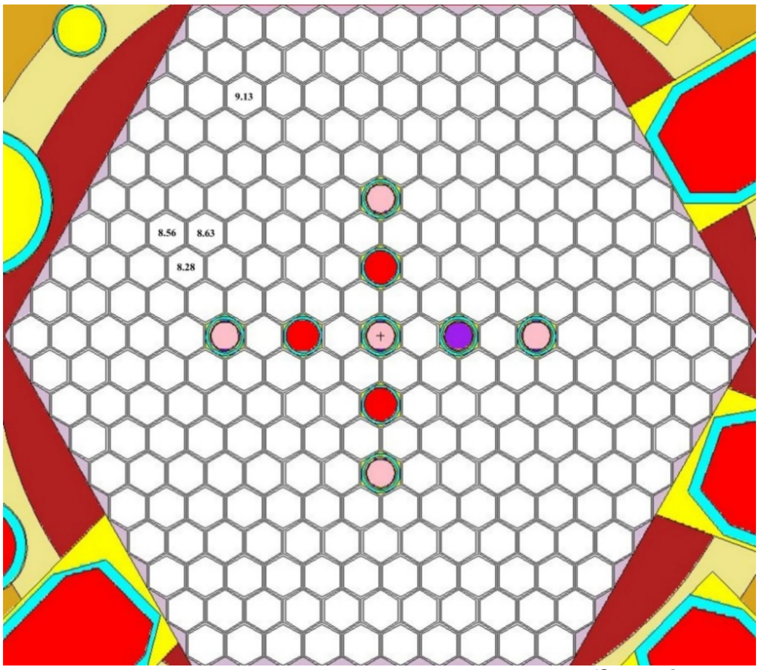

Fig. 8. Total neutron fluxes for variant 2 of channel placement, in units of 10^{13} n/cm^2·s. For irradiation planning, the fast-neutron component (> 0.5 MeV) governing sample damage was used (see the text). (See color Figure on the journal website.)

Thus, variant 2 is preferable due to the smaller difference in neutron flux values within the channels. The core loading map was specifically calculated for this configuration of channel arrangement. The computations indicate that the reactivity margin of the reactor core decreases by $2.7\beta_{eff}$ due to the loading of the experimental channels. In the case of long-term irradiation, such a decrease in the reactivity margin is undesirable. Therefore, it is possible that the final version of the new core loading map will be variant 2, in which the lateral triple assembly is relocated to the upper row, and an additional single fuel assembly is added. Under these conditions, about $0.8\beta_{eff}$ is added to the reactivity margin.

Fig. 9 presents a typical neutron energy spectrum in the experimental channel of the WWR-M research reactor under study, calculated using the MCNP-4C code. The resulting spectrum is consistent with modern theoretical understanding of neutron spectra in thermal nuclear reactors and supports the validity of the numerical simulations performed. In addition, the resulting spectrum is in close agreement with that derived from earlier calculations of the neutron spectrum in the WWR-M reactor [19]. The structure of the spectrum clearly reveals a pronounced peak in the thermal energy region, corresponding to thermal neutrons, as well as a broad plateau in the epithermal energy region and a fast-neutron peak from fission. Because the epithermal spectrum follows approximately a $1/E$ law, the flux per unit lethargy is nearly constant in this region; on a logarithmic energy axis with equal-width bins, this appears as an extended, nearly flat plateau. Thus, the observed energy dependence of the neutron flux reflects the characteristic physics of neutron moderation in the moderator and scattering in structural materials.

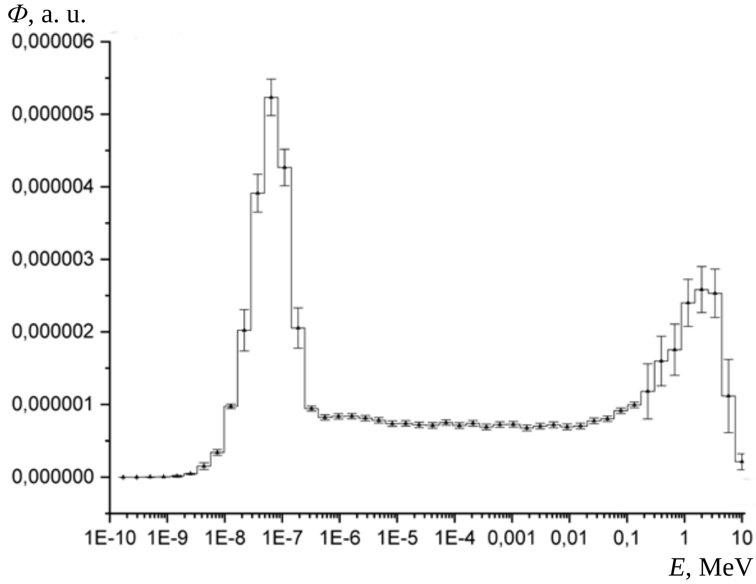

Fig. 9. Neutron energy spectrum in the experimental channel, calculated using MCNP. Energy is shown on a logarithmic scale; flux values are normalized per source particle and given in arbitrary units (a.u.).

Beyond conventional calculations of neutron fluxes and reactor core reactivity, it is essential to evaluate the risk of emergency situations arising during the operation of experimental channels to ensure the safe functioning of all equipment. An example of this type of assessment is presented below for the case of a single channel inserted into the reactor core according to loading scheme 403.

The only possible emergency situation directly related to the experimental channel could be the following. During the irradiation of samples, the channel loses its integrity, allowing water to enter. Since the samples are irradiated at a temperature of approximately 300 °C, all water evaporates almost instantly, resulting in the channel being filled with steam. The temperature of the samples gradually decreases, the amount of water in the channel increases, and the steam density rises until all the steam condenses into water.

Thus, in this case, the initial state of the system is a helium-filled channel, with reactivity close to zero. As the steam density progressively increases, the system's reactivity rises. Table 2 presents the reactivity calculation results depending on steam density. It was assumed here that water enters the channel quickly enough that the emergency protection rods do not have time to activate. The calculation shows that the maximum reactivity of $0.431\beta_{eff}$ is reached at a water density of 0.6 g/cm^3 in the channel. The subsequent kinetics of the process depends on multiple factors, the most significant of which is the rate of water inflow into the channel. Nonetheless, certain estimates can be made under the most conservative assumption that $0.431\beta_{eff}$ reactivity is introduced

Table 2. **Change in reactivity due to water inflow into the experimental channel**

Water density, g/cm^3	0	0.2	0.4	0.6	0.8	1
Reactivity	0.037β_{eff}	0.19β_{eff}	0.336β_{eff}	0.431β_{eff}	0.430β_{eff}	0.419β_{eff}

instantaneously into the reactor core, using the known solutions of the point reactor model equations with constant reactivity and a single group of delayed neutrons. These evaluations will be performed after the final selection of the core configuration with two experimental channels, since the calculations of the maximum reactivity must be performed for the respective core arrangement.

3. Nuclear safety of the spent nuclear fuel storage facility

The WWR-M reactor has three nuclear fuel storage facilities, one of which is designated for fresh fuel storage, while the other two are used for storing irradiated fuel. Spent Fuel Storage Facility No. 2 was attached to the reactor building in 2009 and is intended for storing spent fuel and allowing it to cool before its final transfer beyond the reactor site. The nuclear safety of this facility is substantiated by neutron multiplication factor calculations for an infinite lattice, approved by the nuclear regulatory authority, and does not require reevaluation.

Spent Fuel Storage Facility No. 1 is structurally connected to the reactor and is used both for storing spent fuel and for handling irradiated fuel during reloading and core reconfiguration operations. This storage facility consists of two tiers for storing fuel assemblies, with the second tier structurally composed of sections similar to those used in Storage Facility No. 2. Specifically, the fuel assemblies in the upper tier are arranged in a complex hexagonal lattice, into which neutron-absorbing rods made of boron carbide are embedded. The lower tier is a complex square lattice designed for triple and single fuel assemblies. Both tiers are housed in a tank (or simply, a pool – Fig. 10) filled with distilled water, which provides biological shielding and removes heat from the fuel assemblies through natural convection. The water quality in the storage facility is maintained by an ion-exchange filter. The pool is surrounded by heavy concrete with a thickness of 1.26 m.

The nuclear safety of such a complex two-tier structure cannot be assessed based on neutron multiplication factor calculations for infinite lattices. More specifically, an infinite-lattice approximation is not appropriate here because Storage Facility No. 1 is a finite two-tier tank with pronounced axial leakage, water gaps, and structural heterogeneities (tank walls, support plate), all of which significantly affect k_{eff}. Therefore, we used a full 3-D model with realistic boundary conditions. This challenge led to

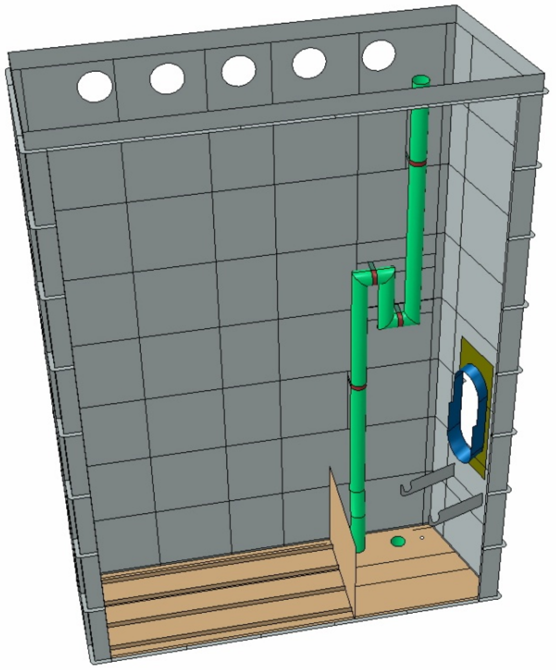

Fig. 10. The model of the tank serving as Storage Facility No. 1 (without the front wall). Four guide rails are positioned at the bottom of the tank to hold a plate containing a lattice of canisters for fuel assemblies. On the right side, a window enables the transfer of fuel assemblies between the reactor and the storage facility. The mechanism for relocating fuel assemblies inside the tank is not shown in the figure. (See color Figure on the journal website.)

the present study, which focuses on evaluating the nuclear safety of the actual fuel assembly configuration in the two-tier Spent Fuel Storage Facility No. 1 and some minor variants. Thus, we evaluate the actual fuel-assembly arrangement implemented at Storage Facility No. 1 after early 2022 (together with minor handling-related variants), with the aim of demonstrating deep subcriticality under realistic boundary conditions.

At present, the second storage tier is not in use. Therefore, the first step is to develop a computational model and calculate the effective neutron multiplication factor for various configurations of fuel assembly loading in the first storage tier.

The calculations were performed using the MCNP-4C code, with the computational model in the first stage incorporating the storage tank (see Fig. 10) and the storage lattice for fuel assemblies, which consists of 96 vertical canisters for triple assemblies and 20 canisters for single assemblies. All canisters are welded to a massive plate made of CAB1 aluminum alloy and mounted at the bottom of the storage tank. A visualization of this computational model, generated using the MCNP-VISED code, is presented in Fig. 11. This figure demonstrates a horizontal cross-section of the lower tier at the mid-height of a fuel assembly. The configuration in Fig. 11 reproduces the actual loading at the time of transfer: 109 single fuel assemblies and two triple fuel assemblies are placed in the first tier in square and linear lattice configurations of canisters, with five canisters left unoccupied. This selection reflects the facility inventory and handling constraints at that time. The red color indicates the presence of water.

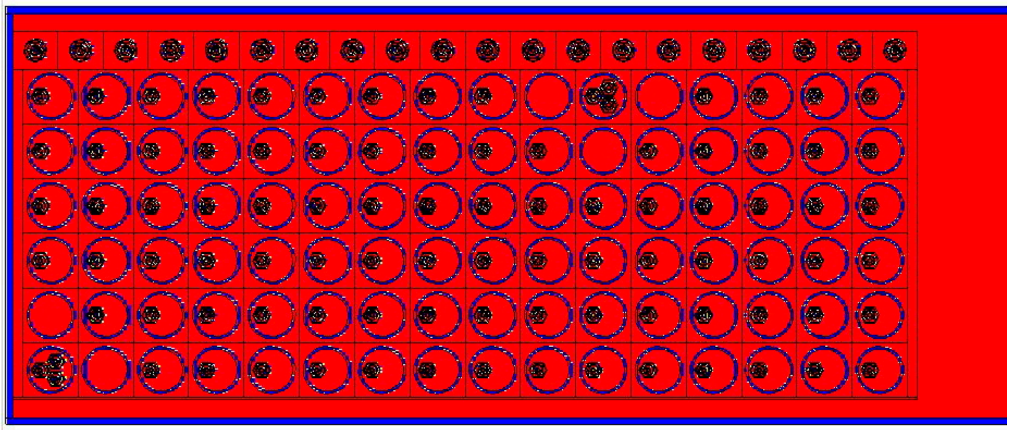

Fig. 11. Visualization of the computational model of Storage Facility No. 1. The actual arrangement of 109 single fuel assemblies and two triple fuel assemblies in square and linear lattice configurations of canisters is shown, with five canisters left unoccupied. (See color Figure on the journal website.)

The results of the MCNP calculations showed that the effective neutron multiplication factor k_{eff} for the given geometric model and the chemical composition of the storage materials is $k_{eff} = 0.401$. This value confirms the deep subcriticality of the system, fully meeting the established nuclear safety requirements. The obtained result demonstrates the subcriticality and safety of the storage facility in its current configuration and filling, with a significant safety margin. It should be noted that all calculations were carried out based on a conservative approach, which assumes unfavorable conditions, including the maximum fuel enrichment. In our calculations, the geometric parameters, such as the distances between assemblies, were assumed to be fixed and consistent with the design features of the storage facility. Let us also remind that the main condition for nuclear safety during the storage of nuclear fuel is the requirement that the maximum effective neutron multiplication factor does not exceed the level of $k_{eff} = 0.95$.

In addition, we performed calculations of the dependence of the effective neutron multiplication factor on the water density in the storage tank, which simulates the onset of an emergency situation. The results of the calculations are presented in Fig. 12. The figure shows that the values of the effective neutron multiplication factor do not exceed $k_{eff} \sim 0.5$ for any water density. Thus, the results confirm the reliability and safety of the storage facility in its current state under both normal and emergency operating conditions. Currently, evaluations of the nuclear safety of Spent Fuel Storage Facility No. 1 are being conducted, taking into account the complete filling of both the first and second storage tiers.

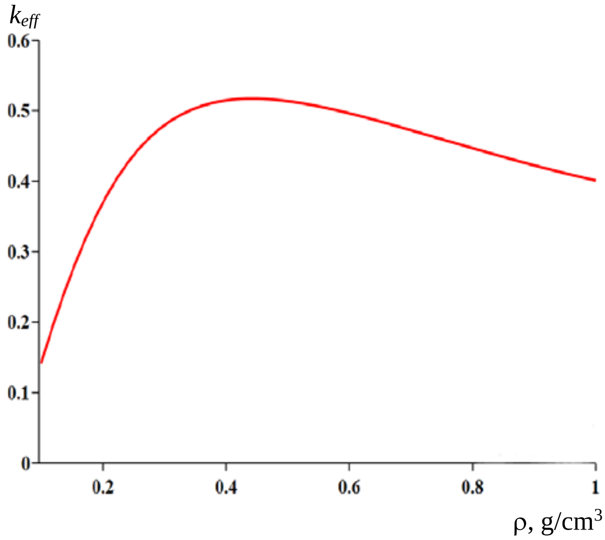

Fig. 12. The dependence of the effective neutron multiplication factor in the spent fuel storage on water density. (See color Figure on the journal website.)

4. Conclusion

We have thoroughly examined and analyzed the activities conducted at the WWR-M research nuclear reactor of the INR of NASU, over the last five years, with a focus on nuclear safety aspects and ongoing research efforts. In 2019–2022, preparations were made for the irradiation of surveillance specimens of nuclear power reactor vessel metals in the vertical channels of the WWR-M reactor, commissioned by NNEC "Energoatom". As part of these efforts, vertical irradiation channels were designed and manufactured, and comprehensive computational modeling studies were conducted to determine the optimal core configuration, the optimal positioning of the channels, neutron fluxes, reactivity parameters, and the required irradiation time for the samples. The theoretical studies were based on numerical modeling using the well-established MCNP-4C neutron-physics code, within which neutron fluxes, system reactivity parameters, and nuclear safety margins were calculated. The main physical parameters were determined for each of the considered reactor core configurations, including the reactivity margin, the control rod worth, as well as the reactivity of the irradiated channels and fuel assemblies. The analysis performed confirmed the feasibility and nuclear safety of the proposed configuration and provided important information for optimizing neutron flux distribution and reactivity control. Furthermore, a comparative analysis of various core configurations confirmed the advantages of the final selected configuration.

However, these research efforts were interrupted in early 2022, leading to the suspension of all operational and research activities at the reactor. The fuel was unloaded and transferred to storage facilities. As a result, a reassessment of the nuclear safety justification for the spent nuclear fuel storage facility was required. Accordingly, the present study reports the results of calculations aimed at providing a detailed evaluation of all relevant aspects and properties. The nuclear safety justification for the storage facility was reevaluated, taking into account the actual arrangement of fuel assemblies relocated from the reactor core. In particular, MCNP-based calculations indicated that for the initial geometric model of Storage Facility No. 1 and the known chemical composition of the materials, the effective neutron multiplication factor of the system is $k_{eff} = 0.401$. This calculated k_{eff} value confirms that the storage facility is a deeply subcritical system and fully meets nuclear safety requirements with a significant margin.

Ongoing research aims to further refine these models and expand the scope of nuclear safety evaluations under various operational conditions. Overall, the present study's findings contribute to the advancement of nuclear safety assessment methodologies in complex conditions and may serve as a foundation for further investigations in the analysis of reactor core characteristics, the optimization of spent nuclear fuel storage processes, and improvements in the operational reliability of research nuclear reactors.

The authors are grateful to I. Ulich for his technical assistance in the preparation of one of the figures.

REFERENCES

1. V.M. Makarovskyi et al. Technical safety justification of the WWR-M research reactor operation. Report No. ТОБ.02-136-15/16/17 (Kyiv, Institute for Nuclear Research of NASU, 2017) 305 p. (Ukr)
2. Proceedings of the Scientific Conference "40 Years of Neutron Research at the WWR-M Reactor", Kyiv, Ukraine, Feb. 10, 2000 (Kyiv, 2000) 57 p. (Ukr)
3. I.M. Vyshnevskyi et al. Development of nuclear technologies in the Institute for Nuclear Research, National Academy of Sciences of Ukraine. Nucl. Phys. At. Energy 15(2) (2014) 195. (Ukr)
4. V.I. Slisenko (Ed.). *Institute for Nuclear Research of NASU. 50 Years of Scientific Research and Achievements* (Kyiv: Institute for Nuclear Research of NASU, 2020) 239 p. (Ukr)
5. M.D. Varentsov et al. Change in the uniformity of neutron-doped silicon during heat treatment. Elektronnaya Tekhnika. Ser. 6. Materialy 2(175) (1983) 77. (Rus)
6. V.I. Borysenko, Yu.F. Piontkovskyi, V.V. Goranchuk. Model of formation of in-core neutron detector signal. Nucl. Phys. At. Energy 17(4) (2016) 364. (Rus)
7. E.U. Grinik et al. Analysis of nickel influence on radiation embrittlement of weld metal of WWER-1000 reactor vessels at Ukrainian NPPs. In: *Problems of Resource and Safety of Operation of Structures, Facilities and Machines* (Kyiv: E.O. Paton Electric Welding Institute of NASU, 2009) p. 261. (Ukr)
8. I.M. Vyshnevskyi et al. *Radiation and Nuclear Technologies in the Institute for Nuclear Research of NAS of Ukraine* (Kyiv: Institute for Nuclear Research of NASU, 2014) 209 p. (Ukr)
9. E.U. Grinik, V.S. Karasev. Reversible reduction in the shear moduli of iron alloys during irradiation. Sov. At. Energy 54 (1983) 184.
10. E.U. Grinik, L.I. Tchirko, V.N. Revka. Master curve analysis methodology in view of the assessment of reactor WWER-1000 vessel integrity. Probl. At. Sci. Technol. 3 (2003) 79. (Rus)
11. O. Grytsenko et al. Implementation of the first stage modernization for single-row container assemblies with surveillance specimens of VVER-1000 reactor pressure vessel metal of SUNPP unit 1. Nucl. Radiat. Safety 3(95) (2022) 27. (Ukr)

12. S. Kotrechko, V. Revka, K. Soroka. A physically based criterion for determining the critical brittleness temperature from Charpy impact tests for PRV steels and welds. Metallofiz. Noveishie Tekhnol. 45(8) (2023) 1015.
13. V. Bukanov et al. Development of approaches to surveillance program implementation during the introduction of FA-WR fuel assemblies at VVER-1000 power units. Nucl. Radiat. Safety 1(101) (2024) 28. (Ukr)
14. S. Kotrechko et al. Radiation hardening and embrittlement of the base and weld metal of VVER-1000 reactor pressure vessels. Int. J. Press. Vessels Pip. 216 (2025) 105528.
15. J.F. Briesmeister (Ed.). MCNP – a general Monte Carlo N-particle transport code. Version 4C. Report No. LA-13709-M (Los Alamos, Los Alamos National Laboratory, 2000) 788 p.
16. P.M. Vorona, V.F. Razbudey. Calculational investigations and analysis of characteristics of research reactor WWR-M as a source of neutrons for solution of scientific and applied tasks. Nucl. Phys. At. Energy 11(1) (2010) 57. (Ukr)
17. V.F. Razbudey. Modeling of the neutron experiments at research reactor WWR-M in the Institute for Nuclear Research, National Academy of Sciences of Ukraine. Nucl. Phys. At. Energy 12(2) (2011) 198. (Rus)
18. V.F. Razbudey. Neutron spectra and fluxes in horizontal channels of research reactor WWR-M while conversion on low-enriched fuel. Nucl. Phys. At. Energy 13(3) (2012) 316.
19. O.G. Diakov et al. Calculation of spectrum and neutron flux density in experimental channels of WWR-M reactor. Nucl. Phys. At. Energy 22(3) (2021) 243.

В. А. Бабенко[1,2,*], В. М. Павлович[1], І. А. Хомич[1], В. І. Слісенко[1], В. В. Тришин[1], О. П. Волох[1]

[1] *Інститут ядерних досліджень НАН України, Київ, Україна*
[2] *Інститут теоретичної фізики ім. М. М. Боголюбова НАН України, Київ, Україна*

*Відповідальний автор: pet2@ukr.net

МОДЕЛЮВАННЯ ОПРОМІНЕННЯ ЗРАЗКІВ ТА ОБҐРУНТУВАННЯ ЯДЕРНОЇ БЕЗПЕКИ ПРИ ДОСЛІДЖЕННЯХ НА ЯДЕРНОМУ РЕАКТОРІ ВВР-М

Аналізуються роботи, проведені на ядерному дослідницькому реакторі ВВР-М Інституту ядерних досліджень НАН України за останні п’ять років, з акцентом на питаннях ядерної безпеки та проведених дослідженнях. У 2019–2022 рр. було виконано підготовчі роботи для опромінення зразків-свідків металів корпусів енергетичних ядерних реакторів у вертикальних каналах реактора ВВР-М за замовленням НАЕК «Енергоатом». Для реалізації цього завдання було спроєктовано та виготовлено вертикальні канали для опромінення зразків, а також проведено розрахункові дослідження з визначення оптимальної конфігурації активної зони, найкращого розташування каналів у ній, розподілу потоків нейтронів та необхідного часу опромінення. Дане дослідження базується на чисельному моделюванні з використанням коду MCNP-4C, у рамках якого було виконано розрахунки для оцінки потоків нейтронів, параметрів реактивності та запасів ядерної безпеки. Для кожної конфігурації було визначено критичні параметри ядерної безпеки, включаючи запас реактивності, ефективність поглинальних стрижнів, реактивність опромінених каналів і окремих паливних збірок. Аналіз підтвердив можливість реалізації запропонованої конфігурації та надав важливу інформацію для оптимізації розподілу потоків нейтронів і контролю реактивності. На початку 2022 р. всі операції на реакторі було припинено, а паливо було вилучене з активної зони та переміщене до сховищ. У зв’язку з цим виникла необхідність удосконалення обґрунтування ядерної безпеки сховища відпрацьованого ядерного палива з урахуванням фактичного розташування паливних збірок. У даній роботі розглядаються аспекти безпеки реактора і оцінюються підходи до вдосконалення обґрунтування зберігання опроміненого палива. Представлено результати серії відповідних розрахунків, які були ініційовані та наразі тривають. Поточне дослідження робить внесок у розвиток методології оцінки ядерної безпеки та є основою для подальших досліджень у цій галузі.

Ключові слова: дослідницький реактор ВВР-М, паливна збірка, ядерне паливо, сховище відпрацьованого ядерного палива.

Надійшла / Received 25.09.2025